A field-induced exchange flip in a spin linear trimer in a coordination polymer of cobalt and melamine.

Ignacio Bernabé Vírseda[1], Alexander Prado-Roller[2], Michael Eisterer [3], Hidetsugu Shiozawa[1,4*]

[1]J. Heyrovsky Institute of Physical Chemistry, Czech Academy of Sciences, Dolejskova 3, 182 23 Prague 8, Czech Republic

[2]Department of Inorganic Chemistry, University of Vienna, Währinger Straße 42, 1090, Vienna, Austria

[3]Atominstitut, TU Wien, Stadionallee 2, 1020 Vienna, Austria

[4]Faculty of Physics, University of Vienna, Boltzmanngasse 5, 1090 Vienna, Austria

*To whom correspondence should be addressed; E-mail: hide.shiozawa@jh-inst.cas.cz & hidetsugu.shiozawa@univie.ac.at

Abstract

A coordination polymer of linear trimeric cobalt and melamine has been synthesized. The magnetic isotherms of violet coloured crystals as long as 400 μm show a field-induced transition in an external field of about 2 T at temperatures below 2 K. It is addressed that by assuming the coexistent positive and negative exchange between the nearest-neighbour spins in the linear trimer, this metamagnetic transition can be understood as a transition from antiferromagnetic to ferromagnetic exchange within each trimeric spin cluster without considering long-range magnetic ordering. Although weak inter-cluster or inter-chain exchange to yield a long-range magnetic order is not excluded as another possible and often attributed origin of metamagnetism in low-dimensional spin systems, the present study demonstrates the significance of the exchange flip within each cluster in clustered spin networks. This paves the way towards the realization of stable, yet swicteable states of a spin trimer in the realm of coordination chemistry.

1 Introduction

Since the subject "molecular magnetism" started in the 1980s, growing expertise has led the discovery of single molecule magnets (SMMs), and single-chain magnets (SCMs) Coordination chemistry provides a fruitful path to desgin coordination bonds between organic ligands and metal ions to create organic–inorganic compounds which include molecular coordination complexes or polymeric structures, such as coordination polymers (CPs) and metal-organic frameworks (MOFs) [1][2].

In the present work, we syntehsis a zigzag coordination polymer of alternating trimeric cobalt-acetate units and melamine double layers, $Co_3(CH_3COO)_3(C_3H_6N_6)_2$, as shown in Fig. 1. Melamine is a rich source for hydrogen bonding and its three-fold molecular structure with three amino groups allows it to construct supramolecular frameworks, despite its low solubility in organic solvents.

Spin trimers can be triangular or linear, and represent perfect cases for spin frustration, quantum spin liquids, and multinuclear molecular magnetism. Many coordination complexes and polymers including MOFs with trimeric spin clusters were reported to exhibit a rich variety of magnetism as results of interplay between intra-trimer and inter-trimer exchange.

The magnetisation isotherm of $Co_3(CH_3COO)_3(C_3H_6N_6)_2$ exhibits a metamagnetic transition in fields about 2 T at temperatures below 2 K. Some coordination complexes and polymers with trimeric transition metals were reported to exhibit field-induced metamagnetic transitions, but typically at much lower temperatures at which the thermal energy becomes lower than the interaction energy of interest (e.g exchange, ligand field), or in much higher magnetic fields in which the Zeeman splitting overcomes the interaction energy. [3]

Only a small number of the trimeric spin systems, metal complexes with linear cobalt dimer or trimer [4] and with triangular Mn [5], and CPs with triangular Fe [6], linear Mn-Ni-Mn [7], triangular Mn [8], were reported to exhibit metamagnetic transitions in similar temperature and magnetic field ranges.

Similar metamagnetic properties were reported for 1D CPs with Fe [9][6] or Co [10][11], and 2D CPs with Co [12], Mn [13], or Ni-Cr [14], with single transition-metal nodes, and often attributed to weak interchain exchange coupling.

In general, field-induced metamagnetic transitions were reported in a wide range of materials from alloys to molecular magnets. Various origins of anomalous staircase magnetism includes ligand-field splitting [15], spin waves [16], spin gaps or spin dimers [17][18], magnetic superlattices [19][20], structural phase transitions [21], and exchange bias. The magnetic superlattices and structural phase transitions reported in magnetic alloys and arrays of magnetic particles, and exchange bias that occurs at boundaries between soft and hard magnets, are not of molecular origin expected for coordination polymers. The ligand-field splitting and spin waves can be observed as staircase magnetism in coordination complexes and polymers, but they are observable at much lower temperatures at which their energies exceed the thermal energy. The transtition from a singlet state to a doublet state in spin gap systems requires much higher magnetic fields.

In the present study, the metamagnetism is attributed to intra-trimer interactions. it is shown that the level crossing expected for a trimeric spin cluster with a negative exchange coupling cannot reproduce the metamagnetism in the respective temperature and field range. Instead, taking both negative and positive exchange into account, both field and temperature profiles of the magnetism can be explained. Although weak inter-trimer exchange remians another possible origin of the metamagnetism, the present work provide a solid foundation for understanding molecular magnetism in clustered spin systems.

2 Results and discussion

2.1 Synthesis

Crystals of $Co_3(CH_3COO)_3(C_3H_6N_6)_2$ were synthesized as follows. 2ml of 0.2 M melamine in a mixture of dimethyl sulfoxide (DMSO) and acetic acid with a volume ratio of (DMSO:acetic acid) = (95:5) and 2 ml of 0.1 M cobalt(II) acetate tetrahydrate in methanol were mixed and sealed in a 10ml glass vial at room temperature and heated in an oven at 50 °C for 24 hours. See the SI1 for more details.

2.2 Crystal morphology

Fig. 1 displays the micrographs of crystals of $Co_3(CH_3COO)_3(C_3H_6N_6)_2$ showing the intense violet color and edgy 3D rhomboid shape.

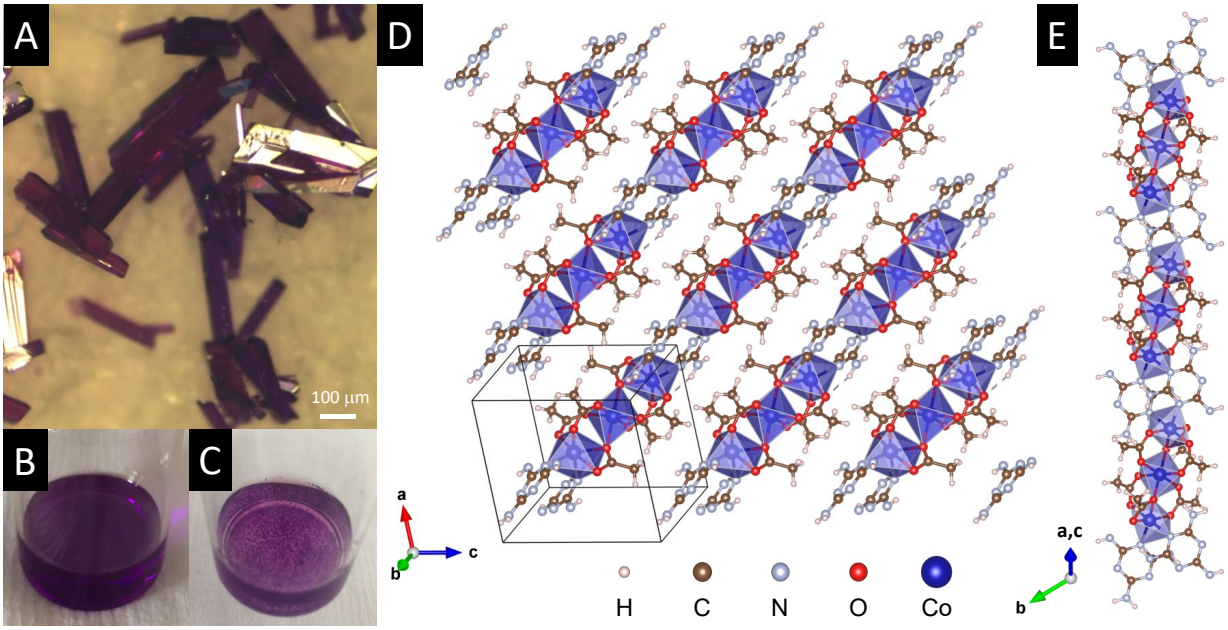

Figure 1: A) Optical micrographs of crystals of $Co_3(CH_3COO)_3(C_3H_6N_6)_2$. B) Photograph of the precursor solution as prepared. C) Photograph of the precursor solution after overnight. D) Lattice structure of $Co_3(CH_3COO)_3(C_3H_6N_6)_2$ viewed normal to the a-c plane. E) Zigzag chain of $Co_3(CH_3COO)_3(C_3H_6N_6)_2$ viewed along the molecular axis of melamine.

2.3 Structure

Single crystal X-ray diffraction analysis of $Co_3(CH_3COO)_3(C_3H_6N_6)_2$ reveals that it is a coordination polymer in which linear trimeric cobalt-acetate units are linked via two melamine molecules to form infinite zigzag chains along the [101] direction, as shown in Fig. 1. [1] Each cobalt atom in the trimeric unit is in an octahedral coordination geometry. The coordination sphere of cobalt in the middle of the trimer (Co2) is composed of six Co-O bonds to six different acetate molecules. The coordination sphere of the two terminal cobalt atoms

[1]CCDC 2215206 contains the supplementary crystallographic data for this paper. These data can be obtained free of charge from The Cambridge Crystallographic Data Centre via www.ccdc.cam.ac.uk/structures

(Co1) is composed of six coordination bonds, which are four Co-O bonds to three different acetate molecules, and two Co-N bonds to the pyridinic nitrogen atoms of two melamine molecules. A narrow angle of 61.07 ° between the two adjacent Co-O bonds to the same acetate molecule leads to a largely distorted octahedral geometry of Co1. See SI2 for more details on the structure analysis. To the best of our knowledge, this coordination polymer has not been previously reported.

2.4 Magnetism

The magnetization isotherms of $Co_3(CH_3COO)_3(C_3H_6N_6)_2$ measured at temperatures of 2, 5, 20, 50, 100, 200 and 300 K are plotted in Fig. 2. At temperatures below 2 K, the staircase profile is prominent with a critical field of abour 2 T. At lower fields, the isotherm follows approximately the Brillouin function for J=1/2 while at high fields it approaches to 3.0 μ_B, the saturation magnetism for the J = 3/2 state. Assuming that the orbital magnetic moment is entirely quenched, this staircase isotherm can be interpreted as a spin transition of cobalt from S = 1/2 to S = 3/2.

2.4.1 Single-ion magnetism

The electronic configuration of divalent cobalt Co(II) is [Ar] $3d^7$. The ligand field strength determines the splitting between the t_{2g} and e_g orbitals in an octahedral geometry. In a weak ligand field, the ground state configuration is ${t_{2g}}^5(e)^2$ resulting in a high spin state with total spin S=3/2. The ground state term of this quartet state is $^4T_{1g}$. A perfect octahedral coordination geometry O_h is hard to realise, and in most cases the octahedron is axially distorted to a tetragonal D_{4h} geometry. An axial elongation causes a splitting of the t_{2g} level to the degenerated low-energy d_{xz} and d_{yz} orbitals, and the high-energy d_{xy} orbital. The e_g level splits into high-energy d_{xz} and low-energy d_{xz}. The corresponding term symbols for the ground and first excited states are $^4A_{2g}$ and ^4E_g, respectively, split by energy Δ. The $^4A_{2g}$ state further splits into two Kramers doublets, $m_s = \pm 1/2$ and $\pm 3/2$, as a result of spin-orbit coupling with zero field splitting (ZFS) energy D. The ground state is $m_s = \pm 1/2$ for D>0 and $m_s = \pm 3/2$ for D<0.

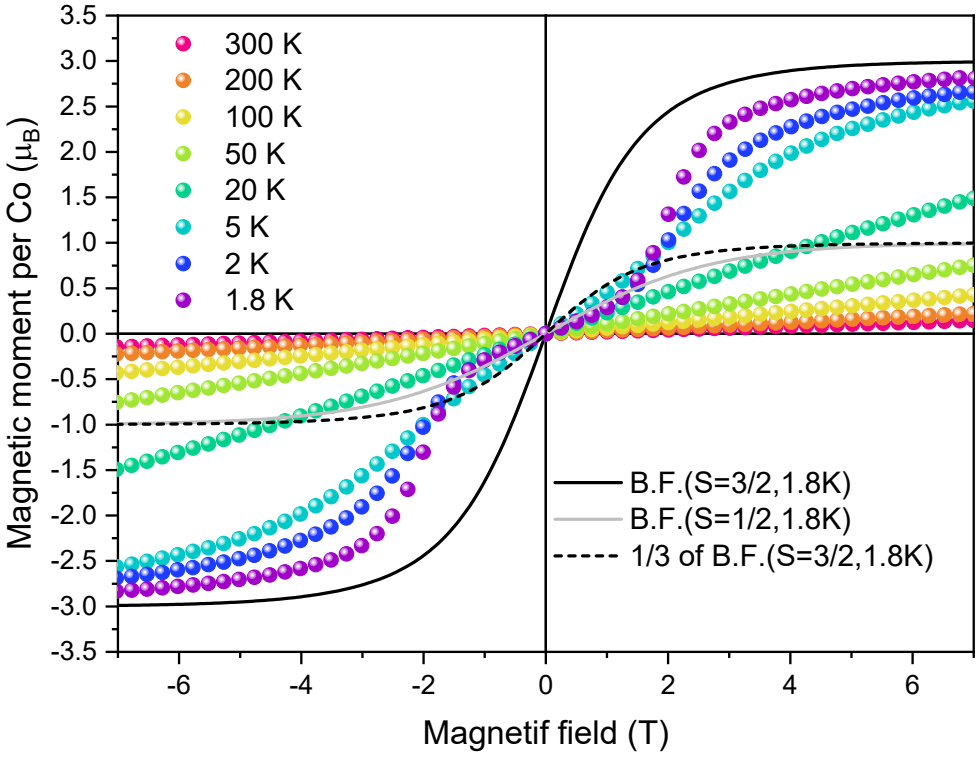

Figure 2: Magnetization isotherms of $Co_3(CH_3COO)_3(C_3H_6N_6)_2$ measured at temperatures of 1.8, 2, 5, 20, 50, 100, 200 and 300 K. The Brillouin functions (B.F.) for S = 3/2 and 1/2 at 1.8 K are plotted as black and grey curves, respectively. The dashed curve is one third of BL for S = 3/2 at 1.8 K.

The spin Hamiltonian taking the zero-field splitting and the first Zeeman term into account is [22]

$$\hat{H}_{zfs} = D[\hat{S}_z^2 - 1/3S(S+1)] + g_{\parallel}\mu_B H_z \hat{S}_z + g_{\perp}\mu_B(H_x\hat{S}_x + H_y\hat{S}_y) \quad (1)$$

where D is the ZFS parameter, $\hat{S}_x$, $\hat{S}_y$ and $\hat{S}_z$ represents spin operators, S is the total spin quantum number, H_x, H_y and H_z are the three scalar components for external magnetic field, $g_{\parallel}$ and $g_{\perp}$ are the g-tensors in the direction parallel and perpendicular to the z axis, μ_B is the Bohr magneton. The second term in the expression is the spin Zeeman term. Considering only the first order Zeeman term, $H_y = H_z = 0$, energy levels E_n for S =3/2 are $\pm\frac{1}{2}g\mu_B H - D$ for $\pm m_S = 1/2$ and $\pm\frac{3}{2}g\mu_B H + D$ for $\pm m_S = 3/2$.

The corresponding partition function is

$$Z_{zfs} = \sum_n e^{-\beta E_n} = e^{\beta D} e^{\frac{1}{2}\beta g \mu_B H} + e^{\beta D} e^{-\frac{1}{2}\beta g \mu_B H} + e^{-\beta D} e^{\frac{3}{2}\beta g \mu_B H} + e^{-\beta D} e^{-\frac{3}{2}\beta g \mu_B H}, \quad (2)$$

where $\beta = -\frac{1}{k_B T}$, and k_B is the Boltzmann constant. Taking only the linear Zeeman term into account, the magnetic moment per cobalt, as the first derivative of the logarithm of Helmholz free energy F with respect to magnetic field H at a given temperature, is given as

$$\begin{aligned} M_{zfs} &= \frac{\partial \beta^{-1} ln Z_{zfs}}{\partial H} = \frac{\beta^{-1}}{Z_{zfs}} \frac{\partial Z_{zfs}}{\partial H} \\ &= \frac{g\mu_B}{2Z_{zfs}} \left[e^{\beta D} e^{\frac{1}{2}\beta g \mu_B H} - e^{\beta D} e^{-\frac{1}{2}\beta g \mu_B H} + 3e^{-\beta D} e^{\frac{3}{2}\beta g \mu_B H} - 3e^{-\beta D} e^{-\frac{3}{2}\beta g \mu_B H} \right]. \end{aligned} \quad (3)$$

Figure 3 shows the magnetization isotherms of $Co_3(CH_3COO)_3(C_3H_6N_6)_2$ at 1.8 K and the fits to Eq. 3 (solid courve). It is apparent that the staircase magnetism observed at 1.8 K cannot be explained by the single-ion model in which the zero-field spliting becomes prominent only at much lower temperatures. Hence, the staircase magnetism with no magnetic hysteresis observed at temperatures as high as a few kelvins can be attributed to exchange coupling among cobalt spins, that can be intratrimer or intertrimer, or both.

2.4.2 Trimeric spins without long-range magnetic order

Here we consider exchange within the trimer. In this scenario, each coblat trimer is in a triplet state (total spin S=3/2) with moderate intra-trimer antiferromagnetic exchange. Inter-trimer exchange coupling is omitted, assuming that both intra- and inter-chain exchanges between trimers are too weak to be discerned in the measured conditions. Possible spin states of the trimer are ↓↓↓, ↑↓↓, ↓↑↓, ↓↓↑, ↑↑↓, ↑↓↑, ↓↑↑, and ↑↑↑. Considering the trimeric structure of mirror symmetry, ↓↓↓, ↓↑↓, ↑↓↑, ↑↑↑ are most likely. The spin Hamiltonian for a trimeric spin system is

$$\hat{H}_{timer} = -2J_{12}\hat{S}_1\hat{S}_2 - 2J_{12}\hat{S}_2\hat{S}_3 - 2J_{31}\hat{S}_3\hat{S}_1, \quad (4)$$

where J_{ij} is the exchange integral between the ith and jth spins, and $\hat{S}_i$ is the spin operator for the ith spin. Assuming $J_{12} = J_{23} = J < 0$ and $J_{31} = \alpha J$, the spin Hamiltonian is reduced to

$$\hat{H}_{timer} = -2J[\hat{S}_1\hat{S}_2 + \hat{S}_2\hat{S}_3 + \alpha\hat{S}_3\hat{S}_1]. \quad (5)$$

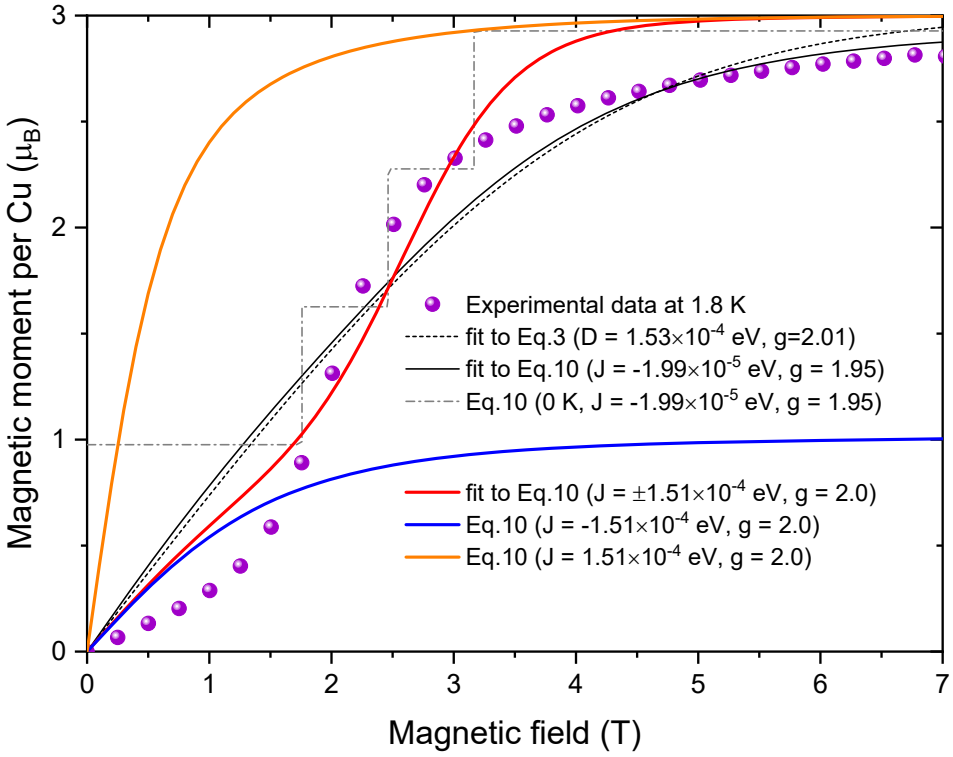

Figure 3: Magnetization isotherms of $Co_3(CH_3COO)_3(C_3H_6N_6)_2$ measured at 1.8 K with the fits to Eq. 3 (dashed curve), Eq. 10 with a negative J (solid curve), and the profile of Eq. 10 at 0 K (dot-dashed profile). The fit to Eq. 10 with bipolar exchange $J = \pm 1.51 \times 10^{-4}$ eV (red curve) and the profiles of Eq. 10 with only negaitve $J = -1.51 \times 10^{-4}$ eV

(blue curve) and only positive $J = 1.51e^{-4}$ eV (orange curve) are also presented.

Introducing $\hat{S}_t = \hat{S}_1 + \hat{S}_2 + \hat{S}_3$ and $\hat{S}_{31} = \hat{S}_3 + \hat{S}_1$ [23], and taking the first Zeeman term into account, we obtain

$$\hat{H}_{trimer} = -J[\hat{S}_t^2 + (1-\alpha)\hat{S}_{31}^2 - \alpha\hat{S}_1^2 - \hat{S}_2^2 - \alpha\hat{S}_3^2] + g\mu_B H\hat{m}_t. \tag{6}$$

Hence, the total energy is given by

$$E(S_t, S_{31}, m_t) = E_0(S_t, S_{31}) + g\mu_B H m_t$$
$$= -2J[S_t(S_t+1) - (1-\alpha)S_{31}(S_{31}+1) - (1-2\alpha)S(S+1)] + g\mu_B H m_t. \tag{7}$$

where $S(S+1)$ is the eigenvalue of $\hat{S}_i^2$ (i = 1,2,3), $S_{31} = 2S, 2S-1, ..., 0$, and $S_t = S_{31} + S, S_{31}+S-1, ..., |S_{31}-S|$, and $m_t = -S_t, -S_t+1, ..., S_t-1, S_t$ is the eigenvalue of the $\hat{m}_t$

The corresponing partition function is

$$Z_{trimer} = \sum_{S_{31},S_t,m_t} e^{-\beta E_0(S_t,S_{31}) + g\mu_B H m_t} = \sum_{S_t,S_{31}} e^{-\beta E_0(S_t,S_{31})} \sum_{m_t=-S_t}^{S_t} e^{-\beta g\mu_B H m_t}. \tag{8}$$

Using formula $\sum_{n=0}^{N-1} r^n = \frac{1-r^N}{1-r}$ results in

$$\begin{aligned} Z_{trimer} &= \sum_{S_t,S_{31}} e^{-\beta E_0(S_t,S_{31})} \frac{e^{\beta g\mu_B (S_t+\frac{1}{2})H} - e^{-\beta g\mu_B (S_t+\frac{1}{2})H}}{e^{\frac{1}{2}\beta g\mu_B H} - e^{-\frac{1}{2}\beta g\mu_B H}} \\ &= \sum_{S_t,S_{31}} e^{-\beta E_0(S_t,S_{31})} \frac{sinh[\beta g\mu_B (S_t+\frac{1}{2})H]}{sinh[\frac{1}{2}\beta g\mu_B H]}. \end{aligned} \tag{9}$$

Then, the magnetic moment of the trimer is

$$\begin{aligned} M_{trimer} &= \frac{\beta^{-1}}{Z_{trimer}} \frac{\partial Z_{trimer}}{\partial H} \\ &= \frac{g\mu_B}{Z_{trimer}} \sum_{S_t,S_{31}} e^{-\beta E_0(S_t,S_{31})} \\ &\cdot \frac{(S_t+\frac{1}{2})cosh[\beta g\mu_B (S_t+\frac{1}{2})H] sinh[\frac{1}{2}\beta g\mu_B H] - \frac{1}{2} sinh[\beta g\mu_B (S_t+\frac{1}{2})H] cosh[\frac{1}{2}\beta g\mu_B H]}{sinh^2[\frac{1}{2}\beta g\mu_B H]} \end{aligned} \tag{10}$$

For a trimer of Co(II) ions, $S = \frac{3}{2}$, and the allowed S_t values are $S_t = \frac{3}{2}$ for $S_{31} = 0$, $S_t = \frac{1}{2}, \frac{3}{2}, \frac{5}{2}$ for $S_{31} = 1$, $S_t = \frac{1}{2}, \frac{3}{2}, \frac{5}{2}, \frac{7}{2}$ for $S_{31} = 2$, and $S_t = \frac{1}{2}, \frac{3}{2}, \frac{5}{2}, \frac{7}{2}, \frac{9}{2}$ for $S_{31} = 3$. Plugging these combinations of S_t and S_{31} into Eq. 10, we get the magnetization per cobalt $M_{Co} = \frac{1}{3} M_{trimer}$ for given H, T, J, α and g. Assuming that J_{13} is negligible, i.e. $\alpha = 0$, to avoid over-parameterization, the magnetisation isotherm can be fit to Eq. 10. The best fit is obtained with $J = -1.94 \times 10^{-5}$ eV (-0.156 cm^{-1}) and $g = 1.96$, the black solid curve in Fig. 3. The fitting curve doesn't show any stepwide feature that corresponds to the level crossing. The grey dot-dashed profile is the calculated magnetisation isotherm at 0 K, exhibiting the three crossing points, $(S_t = \frac{3}{2}, S_{31} = 3, m_t = -\frac{3}{2}) \rightarrow (S_t = \frac{5}{2}, S_{31} = 3, m_t = -\frac{5}{2})$,

$(S_t = \frac{5}{2}, S_{31} = 3, m_t = -\frac{5}{2}) \rightarrow (S_t = \frac{7}{2}, S_{31} = 3, m_t = -\frac{7}{2})$, and $(S_t = \frac{7}{2}, S_{31} = 3, m_t = -\frac{7}{2}) \rightarrow (S_t = \frac{9}{2}, S_{31} = 3, m_t = -\frac{9}{2})$. Again, the model cannot explain the experimental data as the thermal energy at 1.8 K exceeds the Zeeman splitting in the field range where the level crossing occurs.

Next, we assume that both negative and positive exchanges coexist, and all levels are occupied according to the Boltzmann distribution. Figure 4 shows $E(S_t, S_{31}, m_t)$ plotted against the magnetic field with a negative exchange energy of -1.51×10^{-4} eV (-1.22 cm^{-1}) (left panel) and a positive exchange energy of 1.51×10^{-4} eV (1.22 cm^{-1}) (right panel). $E(S_t, S_{31}, m_t)$ for a given combination of S_t, S_{31} with different m_t are plotted in the same colour.

Importantly, the lowest energy level switches from the negative exchange state ($S_t = \frac{3}{2}, S_{31} = 3, m_t = -\frac{3}{2}$) in the left panel to the positive exchange state ($S_t = 9/2, S_{31} = 3, m_t = -\frac{9}{2}$) in the right panel as the field reaches the critical field $\mu_0 H_c$. This transition field depends on the magnitude of exchange coupling J. Figure 5 shows the level crossing with different exchange energies from 1.31×10^{-4} eV to 1.71×10^{-4} eV. The best fit of the experimental magnetic isotherm to the model is obtained with $J = \pm 1.51 \times 10^{-4}$ eV (1.22 cm^{-1}) (red solid curve in Fig. 3). It finally reproduces the step feature near the transition field. The exchange constant is one order greater than $J = -1.94 \times 10^{-5}$ eV (-0.156 cm^{-1}) derived taking only the negative exchange into account. This leads to the level crossing among the negative J states to occur in much higher fields (the first crossing occurs in 13 T as seen in the left panel in Fig. 5) and hence, the same lowest negative J level contributes most to the net magnetism in fields below $\mu_0 H_c$.

Note that the theoretical curve doesn't match the experimental data in the following two respects. First, in fields below the transition field $\mu_0 H_c$, the experimental magnetic moments are smaller than the fitting curve that follows the magnetism of the negative exchange state (blue curve) saturating at about 1.0 μ_B. The reduced magnetic moment can be due to the ZFS. A possible negative ZFS results in the magnetic moment dominated by the kramers doublet in low fields. Secondly, the theoretical curve saturates at about 3.0 μ_B in higher fields, as expected for the S= 3/2 state, while the experimental data is slower to saturate or shows a lower saturation magnetism. This can be due to the orbital magnetic moment, g-factor or

asymmetric exchange, or a combination of them. The linear increase of the magnetism in fields above 4 T is indicative of asymmetric exchange that is expected considering the ligand structure of three cobalt atoms in the trimer.

Figure 6 shows the temperature dependence of the magnetic moment per cobalt for $Co_3(CH_3COO)_3(C_3H_6N_6)_2$ measured in 50 mT, 100 mT, 1 T and 2 T after zero-field cooling (ZFC) and field cooling (FC). The solid curves are the corresponding theoretical data for bipolar exchange $J = \pm 1.51 \times 10^{-4}$ eV. The theoretical curve reproduces the main features of the experimental profiles, specifically, the peak shifting to a lower temperature as the field increases from 1 T to 2 T. The dashed and dot-dashed curves for 1 T and 2 T are cacluated from Eq. 10 with only negative $J = -1.51 \times 10^{-4} eV$ (neg.) and only positive $J = 1.51 \times 10^{-4} eV$ (pos.). In fields well below the transition field $\mu_0 H_c$, the four negative J states of $S_t = \frac{3}{2}, S_{31} = 3$ are at lower energies than the positive J states of $S_t = \frac{9}{2}, S_{31} = 3$, see Fig. 4. At low enough temperatures, the four negative J states of $S_t = \frac{3}{2}, S_{31} = 3$ dictate the net magnetic moment (The boltzmann distribution at 1.8 K in the critical field $\mu_0 H_c$ is plotted in the left panel). As the temperature is raised, the positive J states of $S_t = \frac{9}{2}, S_{31} = 3$ start to be occupied, that increases the net magnetism. This leads to the peak observed in the temperature dependence of the magnetic moments in 1 T and 2 T.

A quantitative analysis of the data requires a more elaborated model taking the crystal field, orbital magnetic moment, spin-orbit coupling and asymmetric exchange into account. Our model is, however, satisfactory within the scope of the present study that is to seek the origin of metamagnetism within each individual cluster.

3 Conclusion

Single crytsals of Co(II) coordination polymer $Co_3(CH_3COO)_3(C_3H_6N_6)_2$ have been synthesized. Linear trimeric cobalt units linked by two melamine molecules offer a model case in which molecular magnetism of clustered spins in a coordination network can be studied. The magnetic isotherm of $Co_3(CH_3COO)_3(C_3H_6N_6)_2$ measured at temperatures below 2 K shows a field-induced transition in a magnetic field about 2 T. It is found that taking the bipolar intra-trimer nearest-neighbour exchange into account, this metamagnetism can be attributed

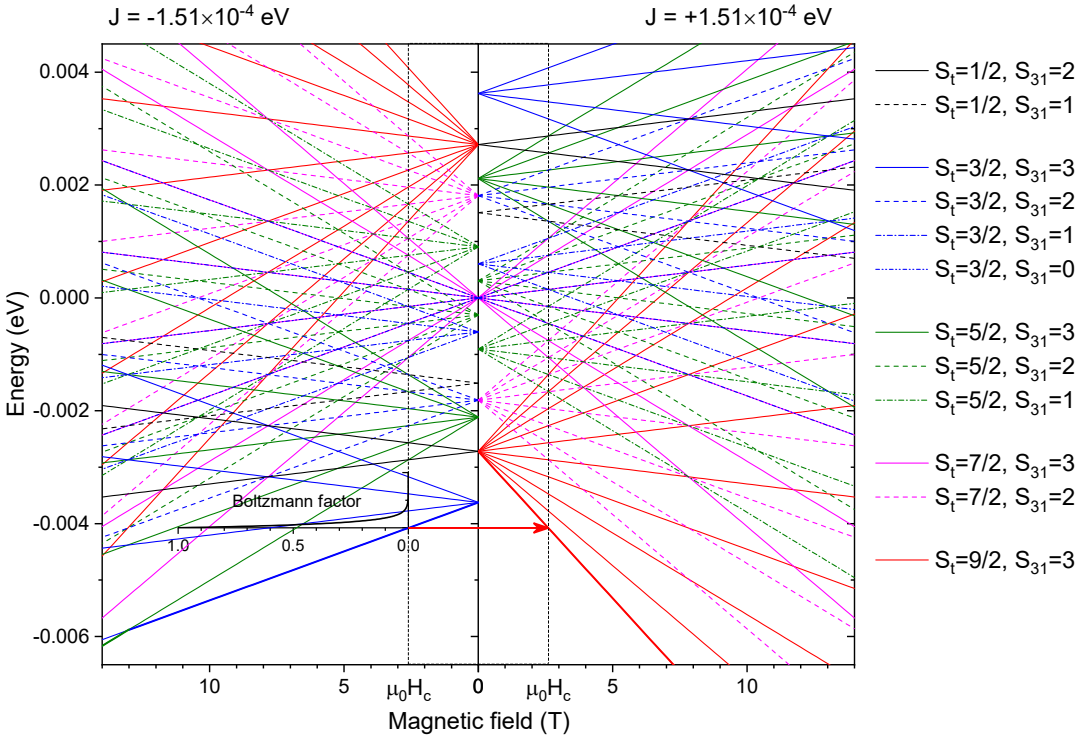

Figure 4: The energy levels $E(S_t, S_{31}, m_t)$ calculated from Eq. 7 for $J = -1.51 \times 10^{-4}$ eV (left panel) and $J = 1.51 \times 10^{-4}$ eV (right panel). The lowerst energy level switches from negative exchange state ($S_t = \frac{3}{2}, S_{31} = 3, m_t = -\frac{3}{2}$ in the left panel) to the positive exchange state ($S_t = \frac{9}{2}, S_{31} = 3, m_t = -\frac{9}{2}$ in the right panel) as the field reaches critical field $\mu_0 H_c$.

predominantly to the properties of exchange-coupled spins within each trimer without long-range magnetic ordering. This work paves the way for a better understanding of molecular magnetism of spin clusters.

Acknowledgements

H. S. acknowledges financial support from the Austrian Science Fund (FWF), project P30431-N36, the Czech Science Foundation (GACR), project 19-15217S and 22-23407S, the Austrian Federal Ministry of Education, Science and Research (BMBWF) and OeAD-GmbH through

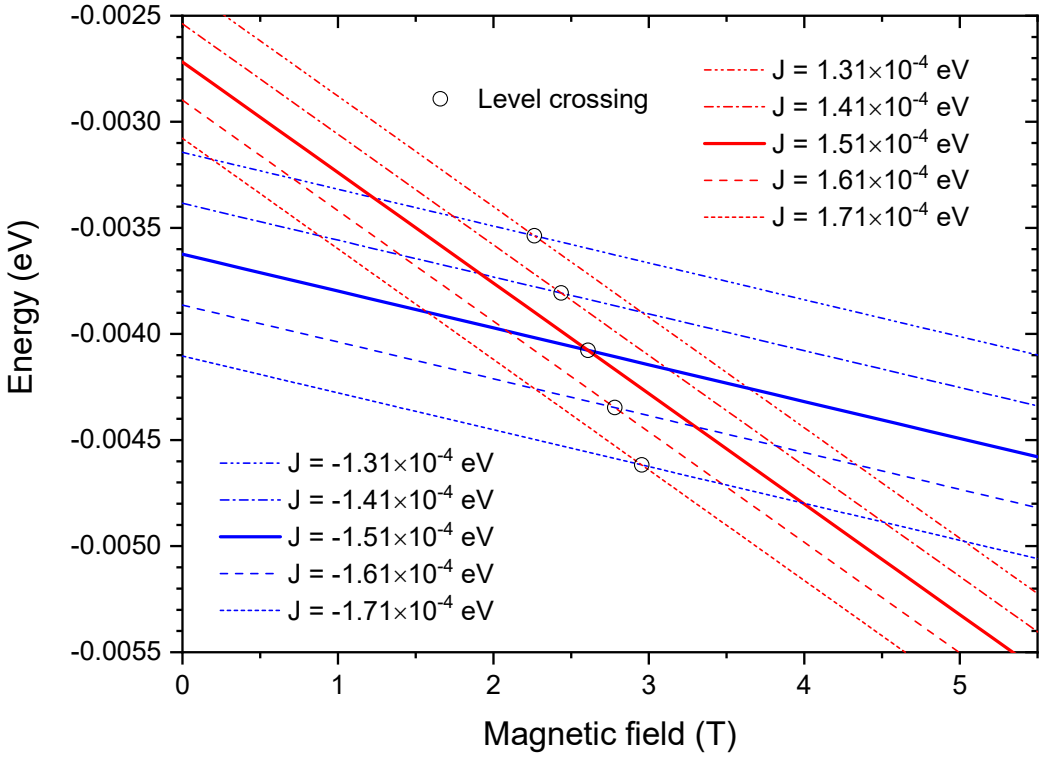

Figure 5: The level crossing points (open circles) between $E(S_t = 3/2, S_{31} = 3, m_t = -3/2)$ with negative exchange (blue) and $E(S_t = 9/2, S_{31} = 3, m_t = -9/2)$ with positive exchange (red) as a function of exchange energy ranging from $\pm 1.31 \times 10^{-4}$ eV to $\pm 1.71 \times 10^{-4}$ eV.

Scientific & Technological Cooperation (WTZ) program, project CZ 18/2019, and the Ministry of Education, Youth and Sports of the Czech Republic (MEYS) through V4-Japan joint research program, project 8F21010. The authors thank S. Loyer and A. Stangl for technical assistance.

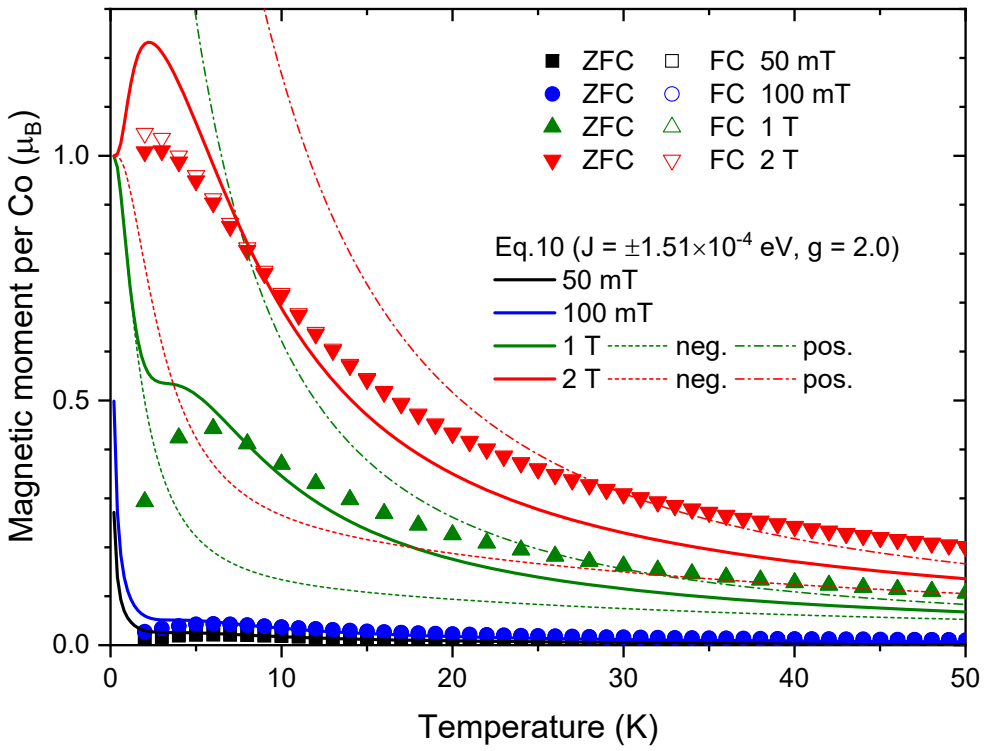

Figure 6: Temperature dependence of the magnetic moment per cobalt atom for $Co_3(CH_3COO)_3(C_3H_6N_6)_2$ measured in fields of 50 mT (black rectangles), 100 mT (blue circles), 1 T (green triangles) and 2 T (red inverted triangles). The solid and open symbols correspond to the data after zero-field cooling (ZFC) and after field cooling (FC), respectively. The solid curves are Eq. 10 for $J = \pm 1.51 \times 10^{-4}$ eV. For 1 and 2 T, the temperature profiles calcuated from Eq. 10 with only negative $J = -1.51 \times 10^{-4}$ eV (neg.) and only positive $J = 1.51 \times 10^{-4}$ eV (pos.) are also plotted as dashed and dot-dashed curves, respectively.

References

[1] Stuart R. Batten, Neil R. Champness, Xiao-Ming Chen, Javier Garcia-Martinez, Susumu Kitagawa, Lars Öhrström, Michael O'Keeffe, Myunghyun Paik Suh, and Jan Reedijk. Terminology of metal–organic frameworks and coordination polymers (iupac recommendations 2013). *Pure and Applied Chemistry*, 85(8):1715–1724, 2013.

[2] Mohamedally Kurmoo. Magnetic metal–organic frameworks. *Chem. Soc. Rev.*, 38:1353–1379, 2009.

[3] Kwang-Yong Choi, Yasuhiro H. Matsuda, Hiroyuki Nojiri, U. Kortz, F. Hussain, Ashley C. Stowe, Chris Ramsey, and Naresh S. Dalal. Observation of a half step magnetization in the Cu_3-type triangular spin ring. *Phys. Rev. Lett.*, 96:107202, Mar 2006.

[4] J. Hudák, R. Boča, Ľ. Dlháň, J. Kožíšek, and J. Moncoľ. Structure and magnetism of mono-, di-, and trinuclear benzoato cobalt(ii) complexes. *Polyhedron*, 30(7):1367–1373, 2011.

[5] Jun Tao, Yuan-Zhu Zhang, Yue-Lin Bai, and Osamu Sato. One-dimensional ferromagnetic complexes built with mniii3o units. *Inorganic Chemistry*, 45(13):4877–4879, 2006. PMID: 16780303.

[6] Qi-Long Wu, Song-De Han, Qing-Lun Wang, Jiong-Peng Zhao, Feng Ma, Xue Jiang, Fu-Chen Liu, and Xian-He Bu. Divalent metal ions modulated strong frustrated m(ii)–fe(iii)3o (m = fe, mn, mg) chains with metamagnetism only in a mixed valence iron complex. *Chem. Commun.*, 51:15336–15339, 2015.

[7] Claude Coulon, Rodolphe Clérac, Wolfgang Wernsdorfer, Thierry Colin, and Hitoshi Miyasaka. Realization of a magnet using an antiferromagnetic phase of single-chain magnets. *Phys. Rev. Lett.*, 102:167204, Apr 2009.

[8] Jun-Liang Liu, Guo-Zhang Huang, and Ming-Liang Tong. Field-induced dynamic magnetic behaviour of a canted weak ferromagnetic chain material. *Inorg. Chem. Front.*, 2:403–408, 2015.

[9] Yan-Zhen Zheng, Wei Xue, Ming-Liang Tong, Xiao-Ming Chen, Fernande Grandjean, and Gary J. Long. A two-dimensional iron(ii) carboxylate linear chain polymer that exhibits a metamagnetic spin-canted antiferromagnetic to single-chain magnetic transition. *Inorganic Chemistry*, 47(10):4077–4087, 2008. PMID: 18422310.

[10] Andrea Caneschi, Dante Gatteschi, Nikolia Lalioti, Claudio Sangregorio, Roberta Sessoli, Giovanni Venturi, Alessandro Vindigni, Angelo Rettori, Maria G. Pini, and Miguel A. Novak. Cobalt(ii)-nitronyl nitroxide chains as molecular magnetic nanowires. *Angewandte Chemie International Edition*, 40(9):1760–1763, 2001.

[11] M. Nandi and P. Mandal. Magnetic and magnetocaloric properties of quasi-one-dimensional ising spin chain cov2o6. *Journal of Applied Physics*, 119(13):133904, 2016.

[12] S. Wöhlert, J. Boeckmann, M. Wriedt, and Christian Näther. Coexistence of metamagnetism and slow relaxation of the magnetization in a cobalt thiocyanate 2d coordination network. *Angewandte Chemie International Edition*, 50(30):6920–6923, 2011.

[13] Xin-Yi Wang, Lu Wang, Zhe-Ming Wang, Gang Su, and Song Gao. Coexistence of spin-canting, metamagnetism, and spin-flop in a (4,4) layered manganese azide polymer. *Chemistry of Materials*, 17(25):6369–6380, 2005.

[14] Hsu-Yen Tang, Gene-Hsiang Lee, Kwai-Kong Ng, and Chen-I Yang. A three-dimensional coordination framework with a ferromagnetic coupled ni(ii)-cro4 layer: Synthesis, structure, and magnetic studies. *Polymers*, 14(9), 2022.

[15] Renaud Ruamps, Luke J. Batchelor, Régis Guillot, Georges Zakhia, Anne-Laure Barra, W. Wernsdorfer, Nathalie Guihéry, and Talal Mallah. Ising-type magnetic anisotropy and single molecule magnet behaviour in mononuclear trigonal bipyramidal co(ii) complexes. *Chem. Sci.*, 5:3418–3424, 2014.

[16] Ratnadwip Singha, Tyger H. Salters, Samuel M. L. Teicher, Shiming Lei, Jason F. Khoury, N. Phuan Ong, and Leslie M. Schoop. Evolving devil's staircase magnetization from tunable charge density waves in nonsymmorphic dirac semimetals. *Advanced Materials*, 33(41):2103476, 2021.

[17] H. Kageyama, K. Yoshimura, R. Stern, N. V. Mushnikov, K. Onizuka, M. Kato, K. Kosuge, C. P. Slichter, T. Goto, and Y. Ueda. Exact dimer ground state and quantized magnetization plateaus in the two-dimensional spin system $srcu_2(bo_3)_2$. *Phys. Rev. Lett.*, 82:3168–3171, Apr 1999.

[18] Yiran Wang, Masayuki Fukuda, Sergey Nikolaev, Atsushi Miyake, Kent J. Griffith, Matthew L. Nisbet, Emily Hiralal, Romain Gautier, Brandon L. Fisher, Masashi Tokunaga, Masaki Azuma, and Kenneth R. Poeppelmeier. Two distinct cu(ii)–v(iv) superexchange interactions with similar bond angles in a triangular "cuv2" fragment. *Inorganic Chemistry*, 61(26):10234–10241, 2022. PMID: 35736661.

[19] T. Matsuda, S. Partzsch, T. Tsuyama, E. Schierle, E. Weschke, J. Geck, T. Saito, S. Ishiwata, Y. Tokura, and H. Wadati. Observation of a Devil's Staircase in the Novel Spin-Valve System SrCo6O11. *Physical Review Letters*, 114(23):236403, jun 2015.

[20] Romana Baltic, Marina Pivetta, Fabio Donati, Christian Wäckerlin, Aparajita Singha, Jan Dreiser, Stefano Rusponi, and Harald Brune. Superlattice of single atom magnets on graphene. *Nano Letters*, 16(12):7610–7615, 2016. PMID: 27779891.

[21] Ryosuke Kainuma, Katsunari Oikawa, Wataru Ito, Yuji Sutou, Takeshi Kanomata, and Kiyohito Ishida. Metamagnetic shape memory effect in nimn-based heusler-type alloys. *J. Mater. Chem.*, 18:1837–1842, 2008.

[22] Olivier Kahn. *Molecular Magnetism*. VCH, New-York, 1993.

[23] Kenjiro Kambe. On the paramagnetic susceptibilities of some polynuclear complex salts. *Journal of the Physical Society of Japan*, 5(1):48–51, 1950.